

**Peptide Functionalization**
How to cite: *Angew. Chem. Int. Ed.* **2021**, *60*, 10850–10857

International Edition: doi.org/10.1002/anie.202016936

German Edition: doi.org/10.1002/ange.202016936

# Efficient Amino-Sulfhydryl Stapling on Peptides and Proteins Using Bifunctional NHS-Activated Acrylamides

Maria J. S. A. Silva, H  lio Faustino, Jaime A. S. Coelho, Maria V. Pinto, Adelaide Fernandes, Ismael Compa  n, Francisco Corzana, Gilles Gasser, and Pedro M. P. Gois\*

**Abstract:** Widely used reagents in the peptide functionalization toolbox, Michael acceptors and *N*-hydroxysuccinimide (NHS) activated esters, are combined in NHS-activated acrylamides for efficient chemoselective amino-sulfhydryl stapling on native peptides and proteins. NHS-activated acrylamides allow for a fast functionalization of *N*-terminal cysteines ( $k_2 = 1.54 \pm 0.18 \times 10^3 \text{ M}^{-1} \text{ s}^{-1}$ ) under dilute aqueous conditions, enabling selectivity over other nucleophilic amino acids. Additionally, the versatility of these new bioconjugation handles was demonstrated in the cross-linking of in-chain or C-terminal cysteines with nearby lysine residues. NHS-activated acrylamides are compatible with the use of other cysteine selective reagents, allowing for orthogonal dual-modifications. This strategy was successfully applied to the late-stage functionalization of peptides and proteins with a PEG unit, fluorescent probe, and cytotoxic agent. The level of molecular control offered by NHS-activated acrylamides is expected to promote amino-sulfhydryl stapling technology as a powerful strategy to design functional bioconjugates.

## Introduction

Novel aqueous chemistries for the selective modification of native peptide chains have been described in recent years and become a key instrument for chemical biology and drug development.<sup>[1]</sup> It is commonly agreed that these tools will provide major insight into basic biology and enable the development of functional bioconjugates with unprecedented properties. To deliver on these promises, it will be key to discover new technologies that offer not only bioconjugation


efficacy, but as importantly, site-selectivity, orthogonality and new mechanisms to control the peptide structure.<sup>[2]</sup>

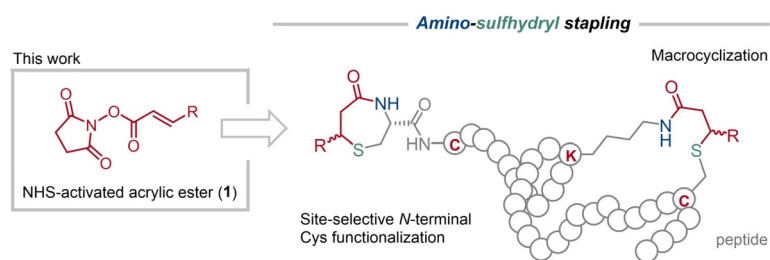
The low abundance of cysteine (Cys) and the high reactivity of the sulfhydryl side chain have made this residue the preferred hotspot to introduce site-selectively modifications on peptide chains.<sup>[3]</sup> However, apart from a few specific reagents that modify *N*-terminal Cys,<sup>[4]</sup> most of the chemistries available to functionalize this amino acid target the reactivity of the sulfhydryl side chain and, for that reason, these methods are often unable to discriminate between different reactive thiol groups on the biomolecule's surface. In addition to this lack of orthogonality, with the notable exception of bridging reagents used in the stapling of disulfide bonds,<sup>[5]</sup> existing chemical methods to modify Cys typically offer poor control over the residue chemical environment, limiting by this way, the manipulation of the peptide chain to improve binding to biological targets, proteolytic stability, among other important pharmacokinetic properties.<sup>[5],6]</sup> Therefore, to further expand the utility of Cys modification for the construction of more complex and well defined bioconjugates, it will be fundamental to devise new Cys modification reactions that offer not only orthogonality but also innovative mechanisms to control the peptide structure.<sup>[7]</sup>

Motivated by this challenge, we envisioned that a chemoselective amino-sulfhydryl stapling reaction would deliver on such prerequisites. The bridging of these functions would enable the bioconjugation to proceed orthogonally at *N*-terminal Cys sites and promote peptide macrocyclization between in chain Cys and a lysine (Lys) close by, which could be explored as a mechanism to control the structure and properties of the bioconjugate. Despite its potential, the amino-sulfhydryl stapling reaction remains underdeveloped<sup>[5f],8]</sup> for bioconjugation applications. Therefore, we set-out to develop a reagent that is capable of stapling amino-sulfhydryl functions with high chemoselectivity, fast kinetic under dilute aqueous conditions and that enables a straightforward structural diversification.

Michael acceptors like carbonyl acrylic reagents reported by the Bernardes group<sup>[9]</sup> and *N*-Hydroxysuccinimide (NHS)-activated esters are among the leading warheads for Cys and *N*-terminus/Lys functionalization, respectively.<sup>[1b]</sup> Therefore, we envisioned that merging these two functional groups in an NHS-activated acrylic ester (**1**) would generate a bifunctional reagent for the selective stapling of amino-sulfhydryl groups (Scheme 1).

[\*] M. J. S. A. Silva, Dr. H. Faustino, Dr. J. A. S. Coelho, M. V. Pinto, Dr. A. Fernandes, Dr. P. M. P. Gois  
Research Institute for Medicines (iMed.Ulisboa)  
Faculty of Pharmacy, Universidade de Lisboa  
Lisbon (Portugal)  
E-mail: pedrogois@ff.ulisboa.pt  
M. J. S. A. Silva, Dr. G. Gasser  
Chimie ParisTech, PSL University, CNRS, Institute of Chemistry for Life and Health Sciences, Laboratory for Inorganic Chemical Biology  
75005 Paris (France)  
Dr. I. Compa  n, Dr. F. Corzana  
Departamento de Qu  mica, Centro de Investigaci  n en S  ntesis Qu  mica, Universidad de La Rioja  
26006 Logro  o, La Rioja (Spain)

 Supporting information and the ORCID identification number(s) for the author(s) of this article can be found under:  
<https://doi.org/10.1002/anie.202016936>

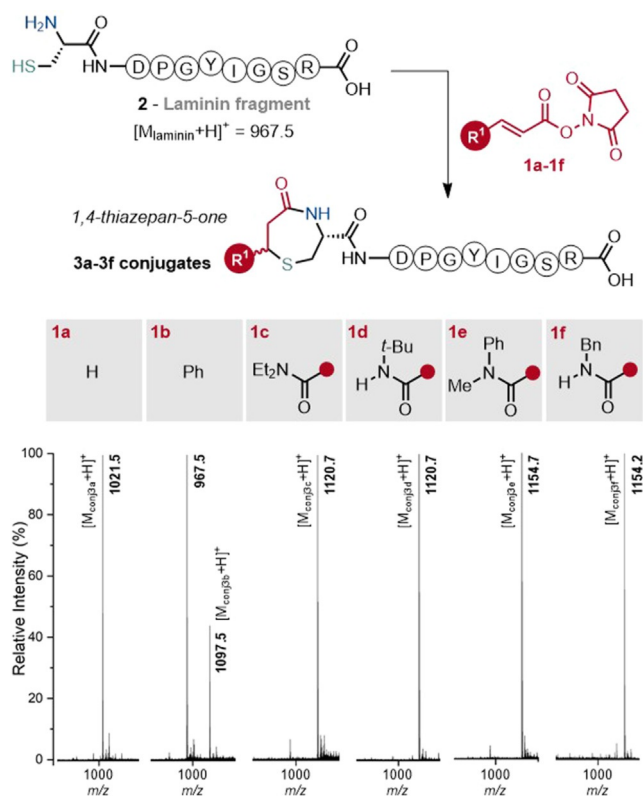


**Scheme 1.** NHS-activated acrylic ester **1** as an amino-sulphydryl stapling reagent in peptides and proteins.

## Results and Discussion

### N-Terminal cysteine functionalization

To test this hypothesis, we evaluated the reactivity of several NHS-activated acrylates featuring different substituents at the  $\beta$ -position (**1a–f**), against a model peptide, laminin fragment, that comprises a *N*-terminal Cys residue. As shown in Scheme 2, while  $\beta$ -phenyl substituted NHS-acrylate (**1b**) offered an incomplete reaction, both unsubstituted NHS-acrylate (**1a**) and NHS-acrylates **1c–1f** with different  $\beta$ -amide substituent profiles, generated very efficiently a 1,4-thiazepan-5-one unit at the peptide *N*-terminal residue



**Scheme 2.** Screening of NHS-activated acrylates **1a–1f** in the reaction with the Laminin fragment and the respective ESI-MS<sup>+</sup> spectra (750–1250 *m/z*) at 5 min reaction time. Conditions: Laminin in ammonium acetate (20 mM, pH 7.0), TCEP (3 equiv), NHS-activated acrylic derivatives (**1a–1f**, 3–10 equiv), 10  $\mu$ M, 37°C. [M<sub>conj3a–3f</sub>+H]<sup>+</sup> is the protonated molecular ion of the corresponding 7-substituted-3-laminin-1,4-thiazepan-5-one products **3a–3f**.

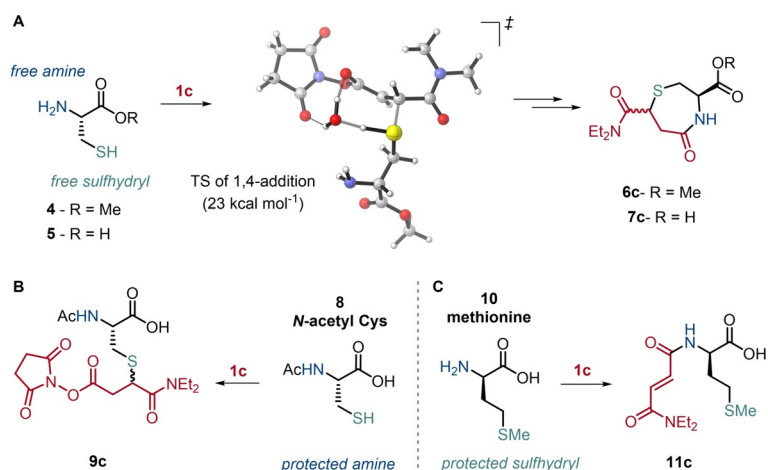
(products **3a**, **3c–3f**; Supporting Information, Section 8, Figures S35–S42).

The formation of this seven-member heterocycle was confirmed by <sup>1</sup>H NMR analysis of the diastereoisomers **6c** and **6c'** obtained in the reaction of Cys methyl ester **4** with NHS-activated acrylamide **1c** (Supporting Information, Sections 3.1.6 and 3.1.7, Figures S1–S3). The diastereoisomer mixture of products was then evaluated in terms of stability in different buffers (pD 9.0, 8.0, 7.0 and 4.5) and in the presence of glutathione. In these conditions, the scaffolds were shown to be stable over one month (Supporting Information, Section 4, Figures S4–S8).

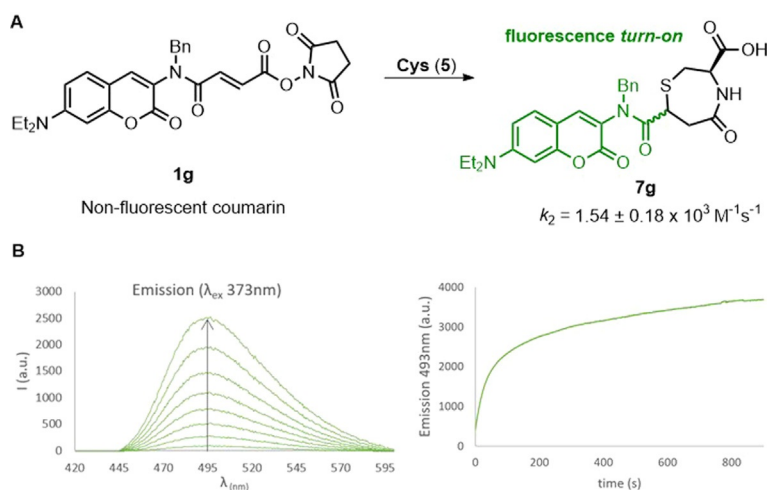
Next, we investigated the mechanism of the 1,4-thiazepan-5-one formation by means of experimental (NMR and ESI-MS) and theoretical (DFT calculations) methods (Scheme 3). For this purpose, we first monitored the reaction of Cys **5** with **1c** by <sup>1</sup>H NMR in deuterated KPi buffer at pD 7.0, at 19 mM and 21°C and by ESI-MS direct injection in ammonium acetate 20 mM, pH 7.0, at 25  $\mu$ M and 37°C (Supporting Information, Sections 5.1 and 5.2, Figures S9–S20). Under both experiment conditions, the reaction generated the expected heterocycle **7c** as the major product (Scheme 3A).

*N*-acetyl Cys **8**, under the same reaction conditions, afforded the 1,4-addition product **9c** (Scheme 3B) as the major product along with the thioester product **S2** (Supporting Information, Section 5.1), while methionine **10** slowly reacted to produce amide **11c** (Scheme 3C). These results suggest that the heterocycle formation is initiated by the thiol-Michael addition that is followed by the intramolecular amidation step. DFT calculations support the formation of the 1,4-thiazepan-5-one product via a thiol-Michael addition-intramolecular amidation sequence with energy barriers of 26 and 12 kcal mol<sup>−1</sup>, respectively. In comparison to this favored sequence, the calculated energy barriers associated with an alternative mechanism involving a thioester formation, *S*-to-*N* transfer and intramolecular thio-Michael addition sequence are higher (31, 34 and 48 kcal mol<sup>−1</sup>, respectively). Furthermore, this second proposed mechanism was discarded as it would result in the preferential formation of a six- over seven-membered heterocyclic ring, which was not observed experimentally (calculated energy barrier of 30 vs. 48 kcal mol<sup>−1</sup> for a 6-exo-trig vs. 7-endo-trig cyclization, Supporting Information, Section 5.3, Figures S21 and S22). Considering these results, we then studied the reaction kinetics by designing a non-fluorescent coumarin NHS-activated acrylamide **1g** that turns-on upon saturation of the conjugated double bond (Scheme 4).<sup>[10]</sup> The reaction of Cys with **1g** under second order conditions, resulted in an emission at  $\lambda_{\text{max}}$  493 nm of **7g** product that enabled to establish a rate constant of  $k_2 = 1.54 \pm 0.18 \times 10^3 \text{ M}^{-1} \text{ s}^{-1}$  for the cyclization (Supporting Information, Section 6, Figures S23–S33, Table S1).

NHS-activated esters are known to cross react with different amino acid nucleophilic side chains.<sup>[1b]</sup> Therefore, we performed the evaluation of the chemoselectivity of NHS-activated acrylamides in a series of experiments. First, **1c** was incubated with an equimolar mixture of Cys and Lys amino acids to test the cross reactivity of the bifunctional reagent



**Scheme 3.** Mechanistic investigations of the 1,4-thiazepan-5-one using model substrates. A) Calculated TS and corresponding  $\Delta G$  in water ( $\text{kcal mol}^{-1}$ ) at the M06-2X/Def2TZVPP//M06-2X/6-31G(d) level of theory using Cys-Me ester as substrate. Conditions: **1c** (1.2 equiv) in KPi (50 mM), pD 7.0/[D<sub>2</sub>]DMSO (4:1), 21 °C and: A) cysteine, 5:1 ratio (1,4-thiazepan-5-one (**7c**):thioester **S2** (Supporting Information, Figure S9); B) *N*-acetyl Cys, 4:1:2 ratio (**9c**:**9c**-COOH:**9c**-thioester); C) methionine, 4:2:1 ratio (**1c**:**11c**:**1c** hydrolyzed). Products observed by NMR spectroscopy (KPi –50 mM pD 7.0) at 5 min reaction time (Supporting Information, Section 5.1).



**Scheme 4.** Kinetic studies for 1,4-thiazepan-5-one formation. A) Coumarin NHS-activated acrylamide **1g** fluorescence turn-on after reacting with Cys. Reactions were performed in second order conditions (equimolar amounts (10  $\mu\text{M}$ ) of coumarin **1g** and Cys) in KPi 50 mM, pH 7.0, 23 °C. B) Full emission spectra (420–600 nm) traced every 10 s for 900 s ( $\lambda_{\text{ex}} = 373 \text{ nm}$ ). C) Emission increase ( $\lambda_{\text{max}} = 493 \text{ nm}$ ) vs. time (s).

with these two nucleophilic residues. This competition experiment afforded a 99:1 mixture of the 1,4-thiazepan-5-one **7c** and the Lys amidation product **S5** (Supporting Information, Section 9.1, Figures S43–S45). The reaction of NHS-activated acrylamide **1c** with Cys-bombesin **35**, that contains a histidine, or with *C*-Ovalbumin **S7**, that exhibits serine and a Lys residues, generated site-selectively the 1,4-thiazepan-5-one at the *N*-terminal Cys (conjugates **S6** and **S8**, Supporting Information, Sections 9.2 and 9.3, Figures S46–S49, Tables S3 and S4).<sup>[1b,11]</sup>

Then, the reactivity profile of NHS-activated acrylamides was tested in the presence of *N*-terminal and in-chain Cys

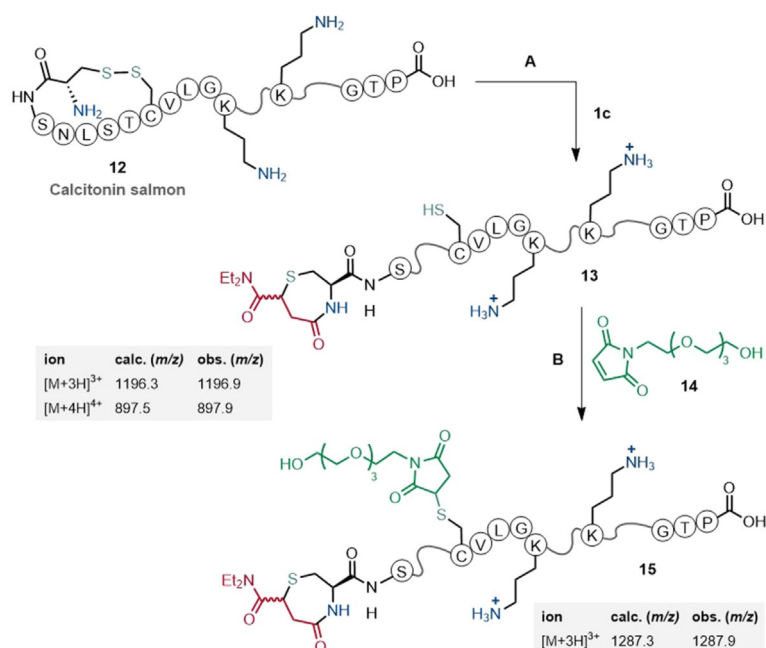
residues using the calcitonin peptide **12**. This 32-amino acid hormone presents a disulfide bond, bridging the *N*-terminal Cys and in-chain Cys (Cys-7). After reducing the disulfide bond with TCEP and decreasing the buffer pH to 4.5, the sequential addition of NHS-activated acrylamide **1c** and PEG-maleimide **14** resulted in the dual site-selective functionalization of calcitonin (product **15**) (Scheme 5; Supporting Information, Section 9.5.2, Figures S56 and S58). The selectivity of NHS-acrylates towards the *N*-terminal Cys position of calcitonin peptide could be confirmed by all-ion-fragmentation (AIF, Supporting Information, Figures S57 and S59). This observation was further corroborated in the competition experiment between Cys (**5**) and *N*-acetylcysteine (**8**) in the presence of **1c**, to provide **7c** with 98% selectivity over *N*-acetylated related products (Scheme 6; Supporting Information, Section 9.4, Figures S50–S53). This selectivity is possibly caused by a synergistic effect of the proximity of thiol to the *N*-terminus amine which presents a lower  $pK_a$ , enhancing the reactivity of this particular position.<sup>[12]</sup>

In these sets of competitive experiments, NHS-activated acrylamides demonstrated to be selective towards the functionalization of the *N*-terminal Cys. Based on these results, we questioned if these reagents could also bridge in-chain or *C*-terminal Cys and nearby Lys residues.

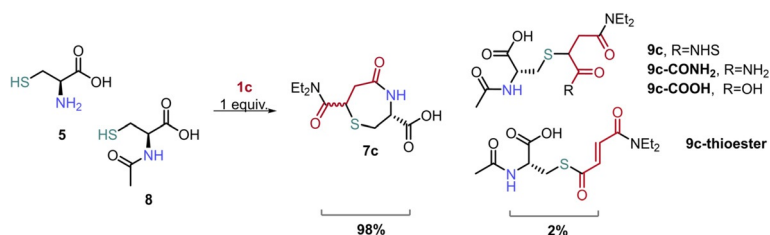
#### Amino-sulfhydryl stapling reaction

To study this macrocyclization, peptides with a *C*-terminal Cys and an internal Lys residue spaced by one, two or three glycine (Gly) residues (peptides **16–18**) were synthesized and reacted with **1f**. As shown in Scheme 7, the stapling reaction proceeded as expected and the macrocycles were isolated and characterized by <sup>1</sup>H NMR, TOCSY-NMR and HRMS (Supporting Information, Section 10, Figures S60–S77). These results were further supported by the reaction of **1f** with a peptide with an acetylated Lys residue (peptide **S1**), in which the macrocycle was not formed (Supporting Information, Section 10.2, Figures S78–S82). With the isolated macrocyclized products we could assess the efficiency of macrocyclization reaction by determining the LC-MS yields under bioconjugation conditions, in ammonium acetate 20 mM, pH 7.0, at diluted conditions (10  $\mu\text{M}$ ) and 25 °C. As shown in Scheme 7, the reaction of **1f** with peptide **16**, with one Gly between the amino and sulfhydryl's groups, was slightly less efficient than the reactions with peptides **17** and **18**, featuring two and three Gly spacers, respectively. This can be explained with stereo constraints imposed by the shorter peptide spacer, that difficult the amidation step (Supporting Information, Section 10.3, Figures S83–S85, Tables S5–S7).





**Scheme 5.** Dual site-selective functionalization of Calcitonin salmon **12** with NHS-activated acrylamide **1c** and maleimide **14**. Conditions: A) Calcitonin in ammonium acetate (20 mM, pH 4.5), TCEP (10 equiv), **1c** (5 equiv), 10  $\mu$ M, 37°C, at 5 min; B) maleimide **14** (10 equiv).



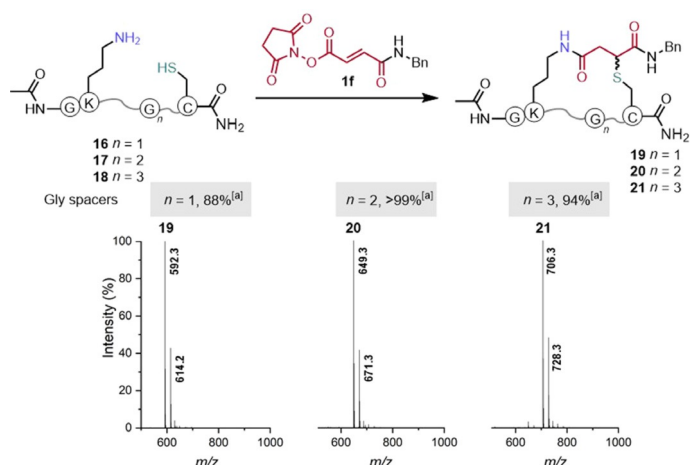
**Scheme 6.** Competition assay of Cys versus *N*-acetyl Cys reaction with NHS-activated acrylamide **1c**. Conditions: Cys (**5**) (2 equiv) and *N*-acetyl Cys (**8**) (2 equiv) in ammonium acetate (20 mM, pH 7.0), **1c** (1 equiv), 50  $\mu$ M, RT, at 5 min. The product ratio was calculated based on the extracted ion current (EIC) chromatogram of LC-HRMS analysis to the reaction crude, showing that 1,4-thiazepane-5-one **7c** was the major product detected by LC-MS. The selectivity is further corroborated by comparison of HPLC UV traces and TIC of the competition assay with control experiments (Figures S52 and S53).

After confirming the possibility to perform the macrocyclization in model peptides, the methodology was applied in the functionalization of the antinucleolin F3 peptide **29** modified with a *C*-terminal Cys. Incubation of this 32-amino acid sequence with 1.5 equiv of NHS-acrylate **1f** resulted in the formation of a mono-modified conjugate **30** that was isolated by semi-preparative HPLC in 89% yield (Scheme 8; Supporting Information, Section 12, Figures S88–S90). The conjugate digestion with trypsin indicated that the stapling occurred between the *C*-terminal Cys and the adjacent Lys residue ( $m/z$   $[M+H]^+ = 437.1853$ ) (Supporting Information, Figure S91, Table S8).

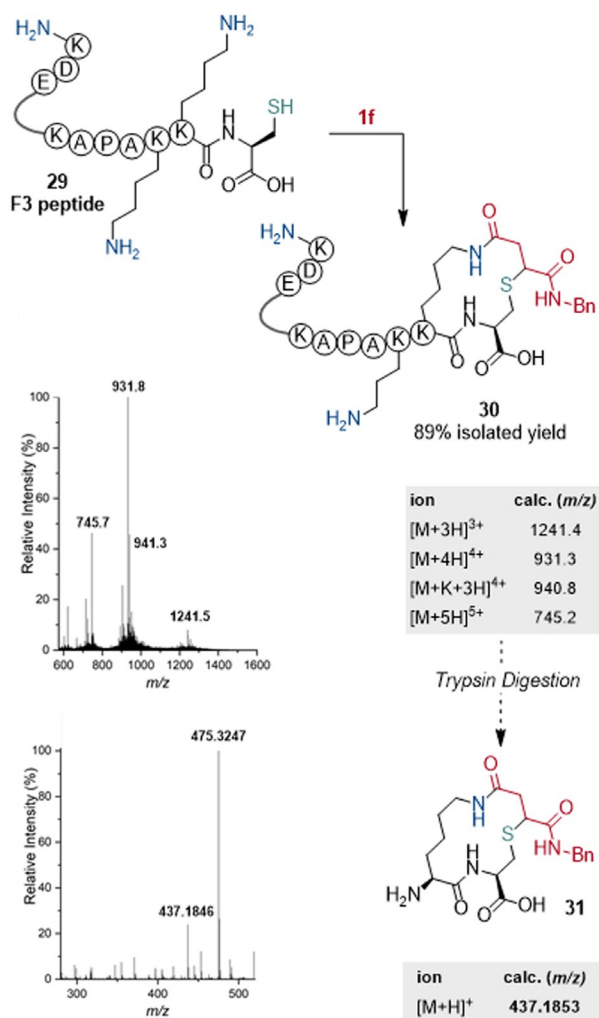
### Orthogonal dual-modification of peptides

Once the amino-sulfhydryl stapling at the *N*-terminal and in-chain sites was established, we tested if these reagents could also engage in the orthogonal functionalization of well-defined peptide **22** featuring a *N*-terminal Cys, a *C*-terminal Cys and an internal Lys residue. This evaluation was initiated with the sequential addition of **1c** (1.2 equiv) and maleimide **23** to the peptide. As shown in Scheme 9, the preference for the *N*-terminal modification over the macrocyclization enabled the straightforward installation of the 1,4-thiazepan-5-one unit (product **S12**) and the subsequent alkylation of the *C*-terminal Cys with the maleimide (conjugate **24**, Supporting Information, Section 11, Figure S86). We then tested if the macrocyclization could also be operated in a similar protocol. Considering the observed preference for the 1,4-thiazepan-5-one formation, we anticipated that to favor the macrocyclization pathway, this mechanism would have to be inhibited, namely by using a *N*-terminal reversible protection group like a boronated thiazolidine.<sup>[4a]</sup> Due to the hydrolysis of **1c** to the corresponding unreactive acid ( $t_{1/2} = 27$  min, Supporting Information, Sections 6.4 and 7, Figures S30–S34, Table S2) and the reversible nature of boronated thiazolidine, the addition of maleimide **23** allowed to intercept the free *N*-terminal Cys and to generate the targeted well-defined conjugate **28**. These complementary strategies offered control over the selective incorporation of a maleimide and an NHS-activated acrylamide orthogonally at different sites.

As abovementioned, at pH 4.5 we could selectively functionalize the *N*-terminal Cys with **1c** in calcitonin salmon peptide **12**. However, conducting the reaction at pH 7.0 and sequentially adding **1c** (10 equiv), we obtained the dual modified product **32** with a 1,4-thiazepan-5-one at the *N*-terminal Cys and a macrocycle between Cys-7 and Lys-11 (Scheme 10, conditions A). More importantly, taking advantage of the relatively fast hydrolysis of NHS-activated acrylamides to generate the unreactive acid functions, we succeeded in orthogonally modifying calcitonin peptide with two distinct NHS-activated acrylamides (dual-modified conjugate **33**). This stepwise protocol involved the selective modification of the *N*-terminal Cys with **1c** at pH 4.5 to generate conjugate **13** (Scheme 10, conditions B), followed by a macrocyclization reaction at pH 7, between Cys-7 and Lys-11 using a different NHS-activated acrylamide **1j** (Scheme 10, conditions C). The identification of these modifications was confirmed by trypsin digestion and by AIF fragmentation (Supporting Information, Section 13, Figures S92–S97, Tables S9 and S10).



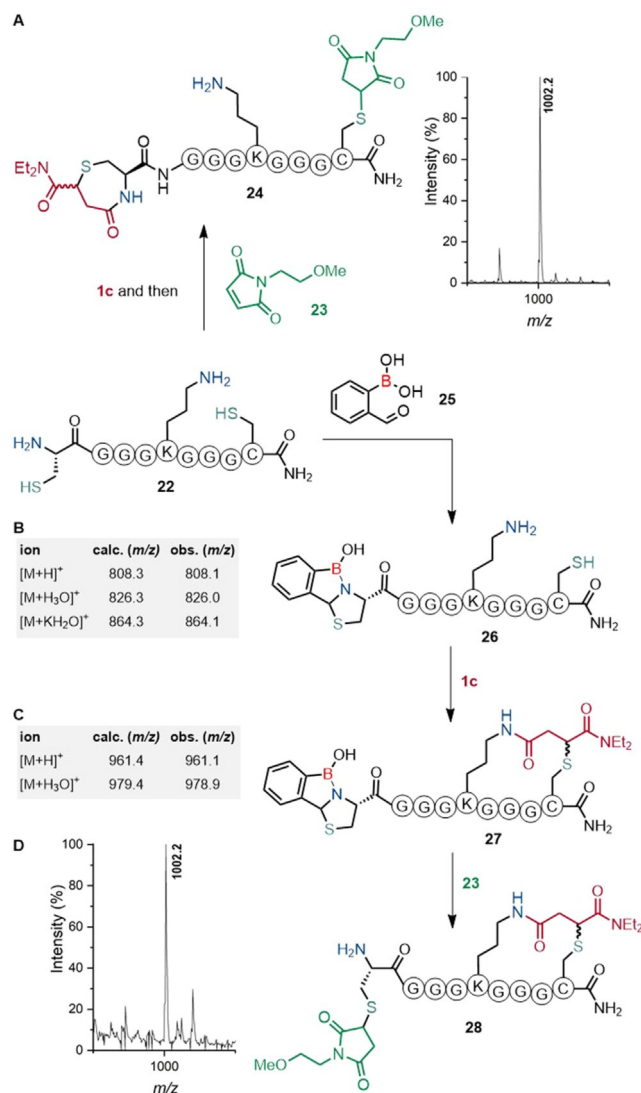
**Scheme 7.** Macrocyclization assays in model peptides with 1 to 3 Gly spacers between in-chain Lys and C-terminal Cys model peptides **16**–**18**. a) yield determined by LC-MS (reactions performed at 10  $\mu$ M) and isolated yields from reactions performed at a concentration of 250  $\mu$ M (21% –**19**; 7% –**20**; 35% –**21**).



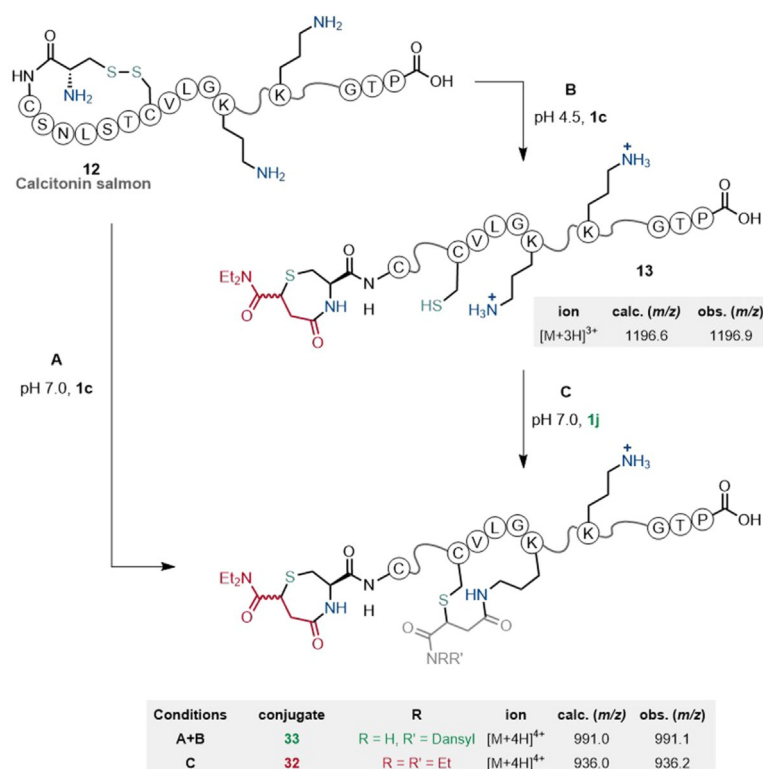
**Scheme 8.** Selective cyclization of F3 peptide with NHS-activated acrylamide **1f** and HRMS of the trypsin digested fragment. Conditions: F3 peptide in ammonium acetate (20 mM, pH 7.0), with **1f** (1.5 equiv), 10  $\mu$ M, 37 °C, 2 h.

## Applications of NHS-activated acrylamides

Considering the observed level of control offered by the NHS-activated acrylamides in the modification of peptide chains, we envisioned that the bis(2,5-dioxopyrrolidin-1-yl) fumarate **34** could further improve the versatility of this platform by permitting the sequential derivatization with nucleophilic amines. To test this protocol, **34** was readily prepared and functionalized with the cytotoxic drug doxorubicin, a PEG unit and a dansyl fluorescent probe, as representatives of nucleophilic amines widely used in the assembly of bioconjugates. These reactions rapidly generated



**Scheme 9.** Orthogonal modification of model peptide **22**. Conditions: A) selective modification of N-terminal Cys with **1c** (1.2 equiv) in ammonium acetate (20 mM, pH 7.0), 10  $\mu$ M, RT, TCEP (10 equiv), followed by the addition of maleimide **23** to the C-terminal Cys to afford conjugate **24**; B) selective modification of N-terminal Cys with **25** (10 equiv) in ammonium acetate (20 mM, pH 7.0), 10  $\mu$ M, RT, TCEP (10 equiv), at 5 min; C) formation of the macrocycle by addition of NHS-activated acrylamide **1c** (15 equiv), at 5 min; D) selective modification of N-terminal Cys with maleimide **23** (10 equiv), at 24 h to afford conjugate **28**.



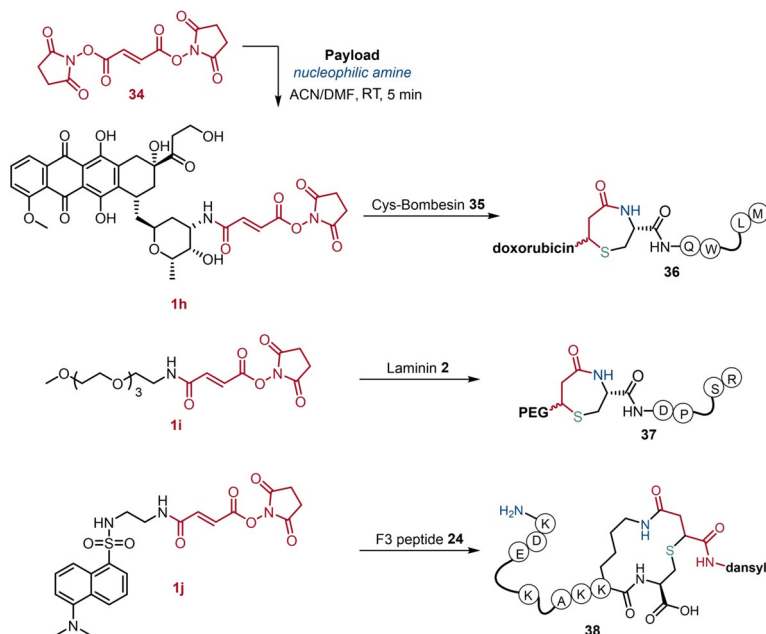
**Scheme 10.** N-terminal and dual site-selective functionalization of Calcitonin salmon **12** with NHS-activated acrylamides. Conditions: A) calcitonin in ammonium acetate (20 mM, pH 7.0), TCEP (10 equiv), **1c** (10 equiv), 10  $\mu$ M, 37°C, at 5 h. B) Calcitonin in ammonium acetate (20 mM, pH 4.5), TCEP (10 equiv), **1c** (5 equiv), 10  $\mu$ M, 37°C, at 5 min; C) pH adjustment to 7.0 with  $\text{NH}_3$  (10%), **1j** (10 equiv), 10  $\mu$ M, 37°C, 1 h.

the targeted NHS-activated acrylamides, which were then used without any purification step in the functionalization of Cys-bombesin **35**, laminin **2** and F3 peptide **29** to prepare the bioconjugates depicted in Scheme 11 in high conversions (Supporting Information, Section 14, Figure S98–S110, Tables S11–S15).

Finally, we performed the amino-sulfhydryl stapling in BSA **39**, a 66 kDa protein, featuring 59 Lys residues and a single free sulfhydryl group of Cys residue (Cys-34, Scheme 12). Remarkably, the conjugation of BSA with 4 equiv of **1j** or 2 equiv of **1g** produced a mixture containing mostly the mono-modified conjugates **40g** and **40j**, along with unmodified BSA **39** and di-modified conjugates **S21g** and **S21j**, indicating, to some extent, cross reactivity with a Lys residue. This solution was then subjected to trypsin digestion, which indicated that the stapling occurred between BSA Cys-34 and Lys-136 (Supporting Information, Section 15, Figures S111–S115).

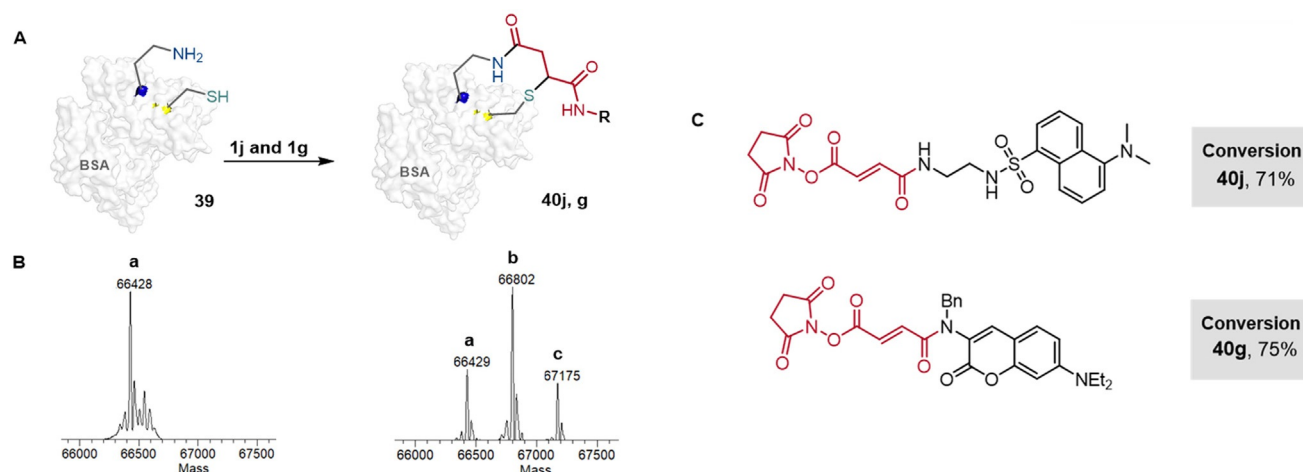
To explain this result, we performed molecular dynamics (MD) simulations on BSA carrying the NHS-activated derivative **1j** at Cys-34 and

examined the distances from all Lys residues to the reactive ester. The two possible diastereomers resulting from the attack of Cys-34 to the acrylamide moiety were also studied. Interestingly, in both conjugates, Lys-136 showed, in average, the lower distance to the reactive center in good agreement with the experimental data. (Supporting Information, Section 16, Figure S116). Additional MD simulations were then performed on BSA **40j** conjugate derivative displaying a (*R*) configuration at the new stereocenter generated in the reaction (Scheme 13). According to the simulations, the average root-mean-square deviation (RMSD) values of the peptide backbone is 4.08 Å. The calculations performed on this system revealed that the installation of **1j** scaffold does not induce any relevant structural modification on the protein. Therefore, we used this fluorescent construct in the labelling of microglia cells. These cells are the resident immune cells of the central nervous system which, among different surveillance duties, protect the brain from foreign proteins. BSA is typically not present in a healthy brain, therefore microglia cells phagocyte this protein, promoting its degradation in the lysosomes.<sup>[15]</sup> Based on this mechanism, the BSA-dansyl conjugate **40j** was studied in the presence of microglia cells, and confocal microscopy



**Scheme 11.** Derivatization of bis(2,5-dioxopyrrolidin-1-yl) fumarate **34** platform with different payloads (doxorubicin **S17**, PEG-NH<sub>2</sub> **S19**, dansyl **S20**) for peptide functionalization. Conditions: first step—nucleophilic amine and **34** in ACN, RT, 5 min at equimolar amount. Second step—peptide fresh solution (1 mg mL<sup>−1</sup>) in ammonium acetate (20 mM, pH 7.0), crude mixture of NHS-activated acrylamides **1h–1j** (1.2 equiv), 10  $\mu$ M, RT, at 5 min. The peptides' conversions (**35** over 99%; **2** over 99%; **24**–89%) were calculated based on the extracted ion current (EIC) chromatogram of LC-HRMS analysis and the conjugates were the major products detected by LC-MS.

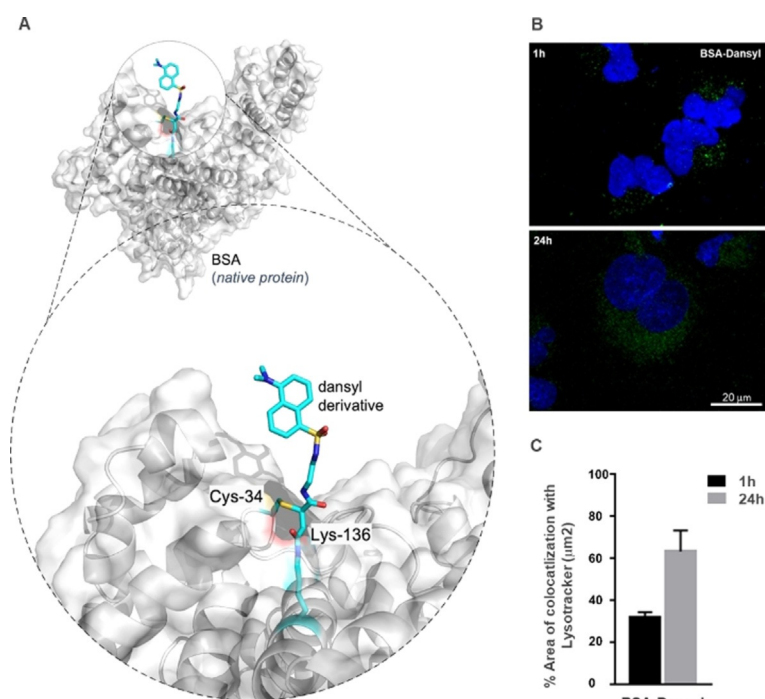




**Scheme 12.** A) Modification of BSA with fluorescent NHS-activated acrylamides **1j** and **1g** in ammonium acetate (20 mM, pH 7.0), 5  $\mu$ M, RT. B) Deconvoluted ESI mass spectrum of BSA (left) and deconvoluted ESI mass spectrum of the reaction mixture with derivative **1j** (right). The spectrum of BSA exhibits the characteristic main peaks assigned to its native form (66428 Da) and to its principal physiological post-translational modifications.<sup>[13]</sup> a) BSA **39**, b) mono-modified BSA conjugate **40j**, c) di-modified BSA with **1j** (**S21j**). Mass spectral deconvolution was performed using a Zscore algorithm in MagTran1.03 software.<sup>[14]</sup> C) Modification of BSA with dansyl-NHS-activated acrylamide **1j** (2 equiv added twice with 1 h intervals) in ammonium acetate (20 mM, pH 7.0), 5  $\mu$ M, RT; and modification of BSA with coumarin-NHS-activated acrylamide **1g** (2 equiv) in KPi (50 mM, pH 7.0), 5  $\mu$ M, RT; respective observed conversions.

images were recorded at 1 h and 24 h after incubation. The experiments clearly support a time dependent uptake of this

conjugate and its accumulation in the lysosomes. These results indicate that this functionalization strategy can be a valuable tool for designing well-defined fluorescent BSA conjugates for lysosome imaging in microglia cells.



**Scheme 13.** A) Representative snapshot derived from 0.5  $\mu$ s MD simulations of BSA-**1j**. Derivative **1j** linked to Cys-34 and Lys-136 is shown in blue and the protein as a white surface. B) Confocal microscopy images of CHME3 microglial cells after incubation with BSA-dansyl conjugate **40j** (5  $\mu$ M diluted in serum-free culture media (green)) for 1 h and 24 h. 4',6-diamidino-2-phenylindole (DAPI (blue)) was used for nucleus labelling after 3 min of incubation. C) Quantitative analysis of BSA-dansyl conjugate **40j** colocalization with microglial lysosomes. After each time point, cells were stained with Lysotracker (yellow), for 30 min, at 37 °C, to observe lysosomes and assess the respective colocalization.

## Conclusion

In summary, NHS-activated acrylamides were shown to be simple and very versatile bioconjugation handles that permit the amino-sulfhydryl stapling in peptides and proteins. The faster reaction kinetics observed for *N*-terminal Cys over other nucleophilic amino acid residues, including in-chain Cys, allowed the selective dual-modification of different Cys residues. Moreover, NHS-activated acrylamides were also successfully applied on in-chain or C-terminal Cys stapling to nearby Lys residues. This bioconjugation strategy involving sustained product stability and fast kinetics under biocompatible conditions, good to full conversion to the desired bioconjugate, is extremely promising in view of applications in biology or medicine. These bifunctional reagents can be easily prepared with diverse and complex payloads requiring minimal manipulation for late-stage bioconjugation of peptides. Finally, the same macrocyclization strategy was applied to BSA protein by stapling free Cys-34 to the nearest Lys-136 as corroborated by MD simulations. The fluorescent BSA-dansyl conjugate was used to label lysosomes in microglia cells. Overall, the versatility demonstrated by NHS-activated acrylamides in the modification of

peptide chains by stapling amino-sulfhydryl groups enlarges the chemical biology toolbox for the construction of functional bioconjugates.

## Acknowledgements

The authors acknowledge financial support from the Fundação para a Ciência e a Tecnologia, Ministério da Ciência e da Tecnologia, Portugal (SFRH/BD/132710/2017, SFRH/BPD/102296/2014, iMed.Ulisboa UIDB/04138/2020 and UIDP/04138/2020; PTDC/QUI-QOR/29967/2017); LISBOA-01-0145-FEDER-029967. We also thank Dr. João N. Rosa for helpful discussions. This work was financially supported by an ERC Consolidator Grant PhotoMedMet to G.G. (GA 681679); G.G. has received support under the program “Investissements d’Avenir” launched by the French Government and implemented by the ANR with the reference ANR-10-IDEX-0001-02 PSL. Funding from the Spanish MCIU (RTI-2018-099592-B-C21 to F.C.) is also acknowledged.

## Conflict of interest

The authors declare no conflict of interest.

**Keywords:** Bioconjugation · esters · macrocyclization · NHS-Activated-Acrylamides · stapling

- [1] a) O. Boutureira, G. J. L. Bernardes, *Chem. Rev.* **2015**, *115*, 2174–2195; b) O. Koniev, A. Wagner, *Chem. Soc. Rev.* **2015**, *44*, 5495–5551; c) A. Maruani, D. A. Richards, V. Chudasama, *Org. Biomol. Chem.* **2016**, *14*, 6165–6178; d) C. D. Spicer, B. G. Davis, *Nat. Commun.* **2014**, *5*, 4740; e) N. Krall, F. P. da Cruz, O. Boutureira, G. J. L. Bernardes, *Nat. Chem.* **2016**, *8*, 103–113; f) E. A. Hoyt, P. M. S. D. Cal, B. L. Oliveira, G. J. L. Bernardes, *Nat. Rev. Chem.* **2019**, *3*, 147–171.
- [2] L. Xu, S. L. Kuan, T. Weil, *Angew. Chem. Int. Ed.* **2021**, <https://doi.org/10.1002/anie.202012034>; *Angew. Chem.* **2021**, <https://doi.org/10.1002/ange.202012034>.
- [3] a) P. Ochtrop, C. P. R. Hackenberger, *Curr. Opin. Chem. Biol.* **2020**, *58*, 28–36; b) S. B. Gunnoo, A. Madder, *ChemBioChem* **2016**, *17*, 529–553; c) J. M. Chalker, G. J. L. Bernardes, Y. A. Lin, B. G. Davis, *Chem. Asian J.* **2009**, *4*, 630–640; d) M. Lahnsteiner, A. Kastner, J. Mayr, A. Roller, B. K. Keppler, C. R. Kowol, *Chem. Eur. J.* **2020**, *26*, 15867–15870; e) S. S. Kulkarni, J. Sayers, B. Premjee, R. J. Payne, *Nat. Rev. Chem.* **2018**, *2*, 0122; f) H. M. Burke, L. McSweeney, E. M. Scanlan, *Nat. Commun.* **2017**, *8*, 15655.
- [4] a) H. Faustino, M. J. S. A. Silva, L. F. Veiros, G. J. L. Bernardes, P. M. P. Gois, *Chem. Sci.* **2016**, *7*, 5052–5058; b) W. Wang, J. Gao, *J. Org. Chem.* **2020**, *85*, 1756–1763; c) H. Ren, F. Xiao, K. Zhan, Y.-P. Kim, H. Xie, Z. Xia, J. Rao, *Angew. Chem. Int. Ed.* **2009**, *48*, 9658–9662; *Angew. Chem.* **2009**, *121*, 9838–9842; d) A. Bandyopadhyay, S. Cambray, J. Gao, *Chem. Sci.* **2016**, *7*, 4589–4593; e) K. Li, W. Wang, J. Gao, *Angew. Chem. Int. Ed.* **2020**, *59*, 14246–14250; *Angew. Chem.* **2020**, *132*, 14352–14356.
- [5] a) N. Assem, D. J. Ferreira, D. W. Wolan, P. E. Dawson, *Angew. Chem. Int. Ed.* **2015**, *54*, 8665–8668; *Angew. Chem.* **2015**, *127*, 8789–8792; b) C. Bahou, D. A. Richards, A. Maruani, E. A. Love, F. Javard, S. Caddick, J. R. Baker, V. Chudasama, *Org. Biomol. Chem.* **2018**, *16*, 1359–1366; c) M. Fernández, A. Shamsabadi, V. Chudasama, *Chem. Commun.* **2020**, *56*, 1125–1128; d) E. A. Hull, M. Livanos, E. Miranda, M. E. B. Smith, K. A. Chester, J. R. Baker, *Bioconjugate Chem.* **2014**, *25*, 1395–1401; e) M. T. W. Lee, A. Maruani, J. R. Baker, S. Caddick, V. Chudasama, *Chem. Sci.* **2016**, *7*, 799–802; f) Q. Lin, D. Hopper, H. Zhang, J. Sfyris Qoon, Z. Shen, J. A. Karas, R. A. Hughes, S. E. Northfield, *ACS Omega* **2020**, *5*, 1840–1850; g) Q. Luo, Y. Tao, W. Sheng, J. Lu, H. Wang, *Nat. Commun.* **2019**, *10*, 142; h) C. Marculescu, H. Kossen, R. E. Morgan, P. Mayer, S. A. Fletcher, B. Tolner, K. A. Chester, L. H. Jones, J. R. Baker, *Chem. Commun.* **2014**, *50*, 7139–7142; i) M. Morais, J. P. M. Nunes, K. Karu, N. Forte, I. Benni, M. E. B. Smith, S. Caddick, V. Chudasama, J. R. Baker, *Org. Biomol. Chem.* **2017**, *15*, 2947–2952; j) T. Wang, A. Riegger, M. Lamla, S. Wiese, P. Oeckl, M. Otto, Y. Wu, S. Fischer, H. Barth, S. L. Kuan, T. Weil, *Chem. Sci.* **2016**, *7*, 3234–3239; k) C. Zhang, P. Dai, A. M. Spokoyniy, B. L. Pentelute, *Org. Lett.* **2014**, *16*, 3652–3655; l) X. Zheng, Z. Li, W. Gao, X. Meng, X. Li, L. Y. P. Luk, Y. Zhao, Y.-H. Tsai, C. Wu, *J. Am. Chem. Soc.* **2020**, *142*, 5097–5103.
- [6] a) A. Tapeinou, M.-T. Matsoukas, C. Simal, T. Tselios, *Biopolymers* **2015**, *104*, 453–461; b) H. Y. Chow, Y. Zhang, E. Matheson, X. Li, *Chem. Rev.* **2019**, *119*, 9971–10001; c) C. J. White, A. K. Yudin, *Nat. Chem.* **2011**, *3*, 509–524.
- [7] a) G. L. Verdine, G. J. Hilinski, *Methods Enzymol.* **2012**, *503*, 3–33; b) L. K. Henchey, A. L. Jochim, P. S. Arora, *Curr. Opin. Chem. Biol.* **2008**, *12*, 692–697; c) Y. H. Lau, P. de Andrade, S.-T. Quah, M. Rossmann, L. Laraia, N. Sköld, T. J. Sum, P. J. E. Rowling, T. L. Joseph, C. Verma, M. Hyvönen, L. S. Itzhaki, A. R. Venkitaraman, C. J. Brown, D. P. Lane, D. R. Spring, *Chem. Sci.* **2014**, *5*, 1804–1809.
- [8] a) M. Todorovic, K. D. Schwab, J. Zeisler, C. Zhang, F. Bénard, D. M. Perrin, *Angew. Chem. Int. Ed.* **2019**, *58*, 14120–14124; *Angew. Chem.* **2019**, *131*, 14258–14262; b) Y. Zhang, Q. Zhang, C. T. T. Wong, X. Li, *J. Am. Chem. Soc.* **2019**, *141*, 12274–12279.
- [9] B. Bernardim, P. M. S. D. Cal, M. J. Matos, B. L. Oliveira, N. Martínez-Sáez, I. S. Albuquerque, E. Perkins, F. Corzana, A. C. B. Burtoloso, G. Jiménez-Osés, G. J. L. Bernardes, *Nat. Commun.* **2016**, *7*, 13128.
- [10] a) Y.-C. Liao, P. Venkatesan, L.-F. Wei, S.-P. Wu, *Sens. Actuators B* **2016**, *232*, 732–737; b) L. Yi, H. Li, L. Sun, L. Liu, C. Zhang, Z. Xi, *Angew. Chem. Int. Ed.* **2009**, *48*, 4034–4037; *Angew. Chem.* **2009**, *121*, 4094–4097.
- [11] P. Cuatrecasas, I. Parikh, *Biochemistry* **1972**, *11*, 2291–2299.
- [12] C. B. Rosen, M. B. Francis, *Nat. Chem. Biol.* **2017**, *13*, 697–705.
- [13] A. Pratesi, D. Cirri, D. Fregona, G. Ferraro, A. Giorgio, A. Merlino, L. Messori, *Inorg. Chem.* **2019**, *58*, 10616–10619.
- [14] Z. Zhang, A. G. Marshall, *J. Am. Soc. Mass Spectrom.* **1998**, *9*, 225–233.
- [15] F. Peri, C. Nüsslein-Volhard, *Cell* **2008**, *133*, 916–927.

Manuscript received: December 21, 2020

Accepted manuscript online: January 29, 2021

Version of record online: April 1, 2021